

Multigigahertz Lumped-Element Electrooptic Modulators

RICHARD A. BECKER

Abstract—Multigigahertz-bandwidth lumped-element optical-guided-wave Mach-Zehnder interferometric modulators have been designed, fabricated in LiNbO₃, tested, and analyzed. Three modulators were built having 3 dB bandwidths of 2.75, 4.4, and 7.3 GHz with V_{π} 's of 7, 14, and 28 V, respectively. A simple RLC equivalent circuit model adequately predicts the packaged modulator performance. Coupled with previously reported work, this demonstrates the ability to reliably design and fabricate lumped-element modulators which operate from dc through 7.3 GHz.

RECENTLY, we reported the development of a series of lumped-element optical-guided-wave interferometric modulators with 3 dB bandwidths from 280 MHz to 2.75 GHz [1]. It was shown that an RLC equivalent-circuit model with a frequency-dependent electrode resistance accurately predicted measured device performance. It was found that electrode and bond wire inductances limited the high-frequency response, especially when the drive source was terminated at the device in 50 Ω . In this letter, extension of this work to wider bandwidths is reported. To increase the bandwidth, the electrode lengths and, thus, capacitances are reduced and no terminating resistor is placed at the input to the device. In addition, a center-tapped electrode structure [1] is used to minimize electrode resistance and inductance. It is shown that the RLC equivalent-circuit model adequately predicts measured device performance for these configurations and for bandwidths up to 7.3 GHz.

The guided-wave Mach-Zehnder interferometric modulator is shown in Fig. 1. The physics of operation is well known [1] and will not be reviewed here. Reference [1] described the equivalent circuit model shown in Fig. 2. Here R_s is the source impedance of the generator, R_e is an effective electrode resistance which is frequency dependent, L is the total inductance of the electrode and bond wires, and C is the electrode capacitance. Because the electrode resistance is distributed down the length of the electrodes, the voltage across the electrodes is spatially varying. The electrooptically induced phase shift is proportional to the spatial integral of the voltage. Accordingly, V_3 is defined as an effective voltage which is proportional to the induced phase shift. The frequency response (FR) of the equivalent circuit is defined as

$$FR = 20 \log \left(\frac{V_3(f)}{V_3(f=0)} \right) \quad (\text{dB})$$

under the condition that V_1 is held constant.

Manuscript received November 16, 1984; revised March 12, 1985. This work was supported by the U.S. Departments of Energy, of the Navy, and of the Air Force.

The author is with Crystal Technology Inc., Palo Alto, CA 94303.

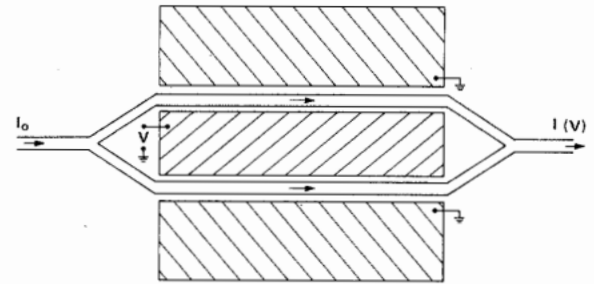


Fig. 1. Guided-wave electrooptic Mach-Zehnder interferometric modulator driven in a push-pull configuration.

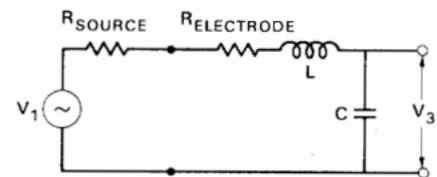


Fig. 2. Lumped-element small-signal circuit model of electrooptic modulator.

This definition of frequency response in terms of electrooptically induced phase rather than output intensity is very useful, because it provides a consistent measure of comparative performance for different types of modulators at different bias points.

The Ti-indiffused LiNbO₃ devices were fabricated by diffusing 400 \AA of Ti into the X face at 1000°C for ≈ 5 h in O₂ bubbled through H₂O. The Ti strip width before diffusion was ≈ 3.8 μm . This set of fabrication parameters yields low-loss waveguides suitable for single TE- and TM-mode propagation at wavelengths in the 0.82–0.86 μm range. After the diffusion, the crystal end faces were cut and polished to facilitate endfire coupling. A 2000 \AA thick buffer layer of pyrolytic SiO₂ was deposited and electron-beam evaporated Cr/Au electrodes with 3.8 μm separation were formed on the interferometer. The center electrode was 35 μm wide and the ground electrodes were 50 μm wide. The Cr/Au metallization thickness was 1.0 μm . Finally, the SiO₂ buffer layer was removed everywhere except directly beneath the electrodes, to avoid any potential problems created by charge transport in the oxide. The modulators are driven in a push-pull mode as shown in Fig. 1, and the r_{33} electrooptic coefficient is being utilized.

Low-frequency measurements were used to determine voltage sensitivity and extinction ratio. The voltage required to drive the modulator output intensity from its maximum to its minimum, V_{π} , was measured by determining the number of intensity maxima that were swept through when a low-frequency ramp voltage of known amplitude was applied. The three devices tested had active

electrode lengths and measured V_π 's of 2, 1, and 0.5 mm and 7, 14, and 28 V, respectively. A figure of merit for the interferometric modulator is the product of V_π and the active electrode length l , $V_\pi l$. For modulators of different length but with the same transverse electrode and waveguide geometry, this product was measured to be $V_\pi l \approx 14 \text{ V} \cdot \text{mm}$. The extinction ratio $10 \log(I_{\max}/I_{\min})$ was determined by measuring the output intensities I_{\max} and I_{\min} with the modulator biased at voltages providing maximum and minimum intensities, respectively. Extinction ratios for the modulators discussed here were in excess of 15 dB.

The values of the circuit elements in the equivalent circuit model were determined by a combination of low-frequency measurements, calculations, and empirical fits. The inductance L is equal to the sum of the calculated bond-wire and electrode inductances. Note that the inductance of the center-tapped electrode shown in Fig. 3 is $\frac{1}{4}$ that for an end-tapped electrode. The value of L is dominated by the bond-wire inductance. The value of C was measured at low frequency. For electrodes with $3.8 \mu\text{m}$ gaps, the capacitance was measured to be $\approx 0.85 \text{ pF/mm}$. This is in good agreement with theoretically predicted values [2]. The effective electrode resistance R_e is given by

$$R_e = GC_1 R(1 + C_2 \sqrt{f})$$

where G is a geometrical parameter which equals 1 for end-tapped electrodes and $\frac{1}{4}$ for center-tapped electrodes. R is the measured end-to-end electrode resistance and C_1 and C_2 are empirical parameters. The resistivity of the $1 \mu\text{m}$ thick Cr/Au metallization was $2.25 \times 10^{-6} \Omega \cdot \text{cm}$, very close to the value of $1.98 \times 10^{-6} \Omega \cdot \text{cm}$ for bulk Au.

To achieve consistent wide-bandwidth response, high-speed packaging techniques were used. Fig. 4 shows a photograph of the packaged 2 mm long device. Evident in the photograph are the gold ribbon bonds and the 50Ω microstrip waveguide which connects the external SMA connectors to the devices. As discussed in [1], the frequency response can be accurately measured by means of a small-signal swept-frequency technique [3]. Fig. 5(a)–(c) shows the linear small-signal frequency response of the 2, 1, and 0.5 mm long devices, respectively. The element values used in the equivalent-circuit model are given in each figure. Notice that the capacitances scale roughly with electrode length, as do the resistances. The inductances are constant due to the fixed length of Au ribbon used in packaging, which is the dominating inductance. The same values for C_1 and C_2 ($C_1 = 0.167$, $C_2 = 1 \times 10^{-4}$) have been used to fit the frequency response of all the devices in this and our earlier paper [1]. As is seen in Fig. 5(a)–(c), the measured frequency response is reasonably smooth and adequately predicted by the RLC equivalent circuit model. The 3 dB frequency points for the three modulators are 2.75, 4.4, and 7.3 GHz, respectively.

The large V_π 's for these modulators are, of course, due to their short lengths which are needed to reach the measured bandwidths. If one is willing to go to the complexity

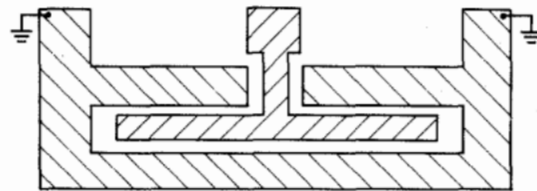


Fig. 3. Schematic of center-tapped electrode for Mach-Zehnder interferometer.

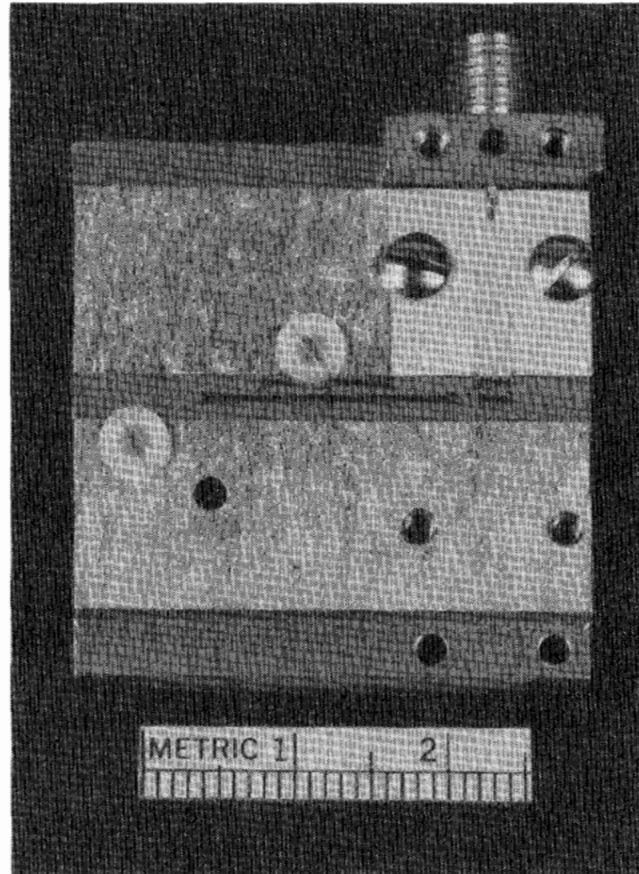


Fig. 4. Photograph of packaged electrooptic modulator.

of a traveling-wave device, then V_π for wide-bandwidth devices can be decreased dramatically [4], [5]. However, the development of these lumped-element devices, coupled with previously reported work [1], does demonstrate the capability to accurately design and fabricate lumped-element electrooptic modulators in Ti-indiffused LiNbO_3 which operate at frequencies in excess of 7 GHz.

In summary, lumped-element electrooptic modulators have been developed in LiNbO_3 with linear small-signal 3 dB bandwidths as wide as 7.3 GHz. An RLC equivalent circuit model is seen to adequately predict performance over the full frequency range.

ACKNOWLEDGMENT

The author wishes to thank R. C. Williamson for many helpful discussions, K. E. Crowe for LiNbO_3 fabrication, and H. V. Roussel for device packaging, testing and computer simulation.

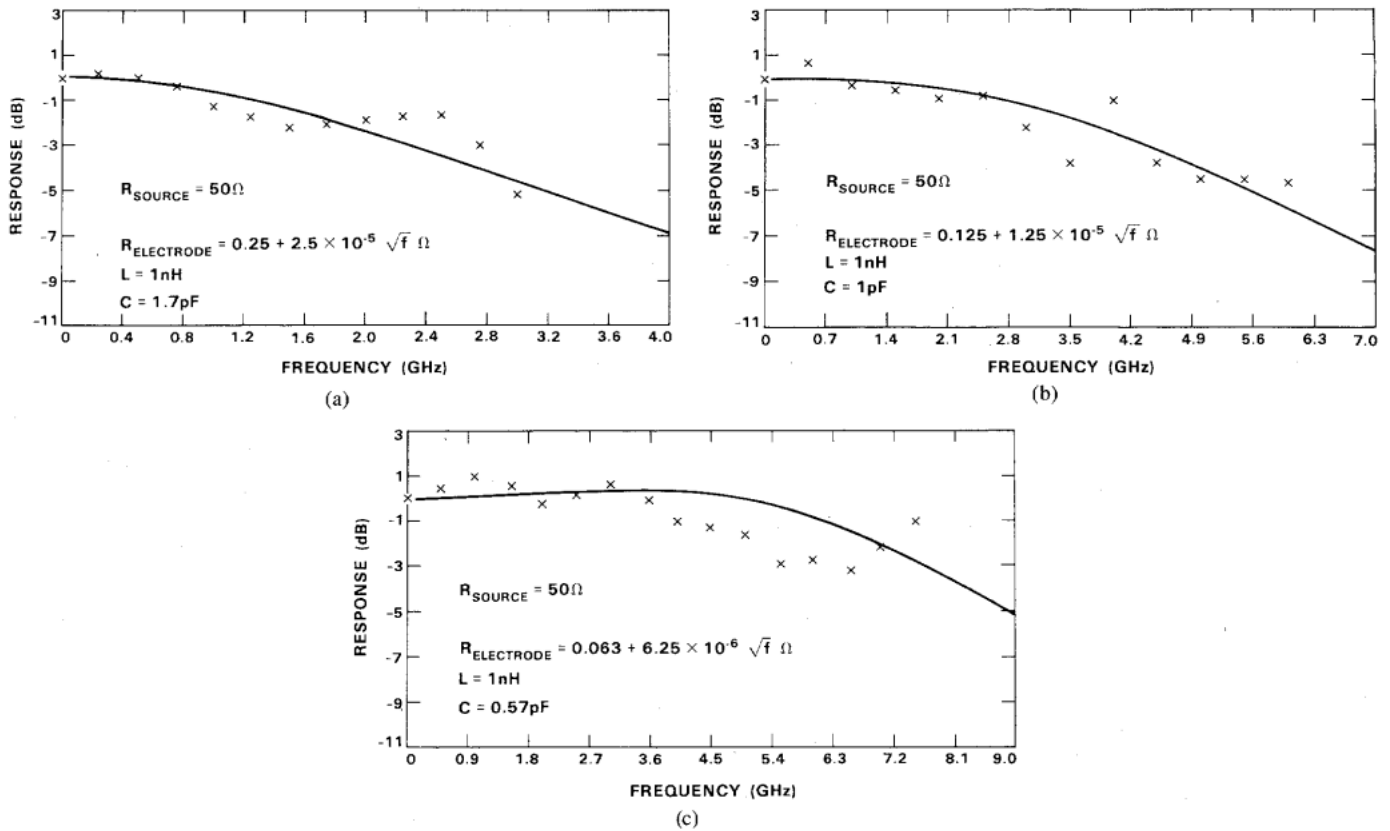


Fig. 5. Measured (X's) and predicted frequency response of modulators with (a) 2 mm long electrode, (b) 1 mm long electrode, and (c) 0.5 mm long electrode. The measured and calculated circuit model element values [1] are given on each graph.

REFERENCES

- [1] R. A. Becker, "Broad-band guided-wave electrooptic modulators," *IEEE J. Quantum Electron.*, vol. QE-20, pp. 723-727, 1984.
- [2] F. Auracher and R. Keil, "Design considerations and performance of Mach-Zehnder waveguide modulators," *Wave Electron.*, vol. 4, pp. 129-140, 1980.
- [3] S. Uehara, "Calibration of optical modulator frequency response with application to signal level control," *Appl. Opt.*, vol. 17, pp. 68-71, 1978.
- [4] R. C. Alferness, "Waveguide electrooptic modulators," *IEEE Trans. Microwave Theory Tech.*, vol. MTT-30, pp. 1121-1137, 1982.
- [5] R. A. Becker, "Traveling-wave electrooptic modulator with maximum bandwidth-length product," *Appl. Phys. Lett.*, vol. 45, pp. 1168-1170, 1984.